

Muon spin relaxation and nonmagnetic Kondo state in PrInAg₂

D. E. MacLaughlin

*Los Alamos National Laboratory, Los Alamos, New Mexico 87545
and Department of Physics, University of California, Riverside, California 92521-0413*

R. H. Heffner

MS K764, Los Alamos National Laboratory, Los Alamos, New Mexico 87545

G. J. Nieuwenhuys

Kamerlingh Onnes Laboratorium, Leiden University, 2500 RA Leiden, The Netherlands

P. C. Canfield

Ames Laboratory and Department of Physics and Astronomy, Iowa State University, Ames, Iowa 50011

A. Amato and C. Baines

Paul Scherrer Institute, CH-5232 Villigen, Switzerland

A. Schenck

Institut für Teilchenphysik, Eidgenössische Technische Hochschule-Zürich, CH-5232 Villigen, Switzerland

G. M. Luke,* Y. Fudamoto, and Y. J. Uemura

Department of Physics, Columbia University, New York, New York 10027

(Received 17 September 1998; revised manuscript received 19 July 1999)

Muon spin relaxation experiments have been carried out in the Kondo compound PrInAg₂. The zero-field muon relaxation rate is found to be independent of temperature between 0.1 and 10 K, which rules out a magnetic origin (spin freezing or a conventional Kondo effect) for the previously observed specific-heat anomaly at ~ 0.5 K. At low temperatures the muon relaxation can be quantitatively understood in terms of the muon's interaction with nuclear magnetism, including hyperfine enhancement of the ¹⁴¹Pr nuclear moment at low temperatures. This argues against a Pr³⁺ ground-state electronic magnetic moment, and is strong evidence for the doublet Γ_3 crystalline-electric-field-split ground state required for a nonmagnetic route to heavy-electron behavior. The data imply the existence of an exchange interaction between neighboring Pr³⁺ ions of the order of 0.2 K in temperature units, which should be taken into account in a complete theory of a nonmagnetic Kondo effect in PrInAg₂.

I. INTRODUCTION

In a seminal paper, Yatskar *et al.*¹ reported evidence for unconventional heavy-fermion behavior in the praseodymium-based intermetallic PrInAg₂. This compound is one of only a handful of Pr-based materials that exhibit heavy-fermion or Kondo-like properties. Specific-heat, magnetic-susceptibility, and neutron-scattering experiments² indicate a non-Kramers doublet (Γ_3) ground state due to crystalline-electric-field (CEF) splitting of the Pr³⁺ ¹H₄ term. The Γ_3 state is *nonmagnetic*, i.e., there are no matrix elements of the magnetic-moment operator within its doubly degenerate manifold. A nonmagnetic ground state would make the heavy-fermion-like specific-heat anomaly found below 1 K and the enormous low-temperature Sommerfeld specific-heat coefficient $\gamma(T) \approx 6.5$ J mole⁻¹ K⁻² quite unexpected, and suggests that PrInAg₂ may be a system in which an unusual nonmagnetic path to heavy-fermion behavior is realized.¹ But such a scenario depends crucially on the nonmagnetic nature of the ground state.

This paper reports two results of muon-spin-relaxation

(μ SR) experiments in PrInAg₂ which support the conclusion of Yatskar *et al.*¹ that the Kondo effect in PrInAg₂ is nonmagnetic in origin. First, we observe no anomaly in the positive-muon (μ^+) relaxation rate in the neighborhood of 1 K, contrary to what would be expected if the specific-heat anomaly involved magnetic degrees of freedom. Second, the temperature and field dependence of the μ^+ relaxation function indicate that the μ^+ relaxation is dominated by dipolar coupling to nearby ¹¹⁵In and ¹⁴¹Pr nuclear magnetic moments (Ag nuclear moments are negligible in comparison). There is no sign of the additional μ^+ relaxation that would be expected from Pr³⁺ local magnetic moments. Furthermore, the observed relaxation behavior below ~ 10 K agrees quantitatively with that expected in the presence of strong *hyperfine enhancement* of the ¹⁴¹Pr nuclear magnetism. Hyperfine enhancement is an effect of the hyperfine coupling between the nucleus and the Van Vleck susceptibility of a non-Kramers *f* ion in a nonmagnetic ground state,³ and only occurs when the Pr³⁺ CEF ground state is nonmagnetic.⁴ Our μ SR results unambiguously establish the nonmagnetic *f*-electron ground state necessary for unusual nonmagnetic heavy-fermion behavior.¹

The remainder of this introduction contains three brief pedagogical sections: a description of the theoretical basis for a nonmagnetic Kondo effect (Sec. I A), an introduction to the elements of the μ SR technique used in this study (Sec. I B), and a review of the important aspects of hyperfine enhancement (Sec. I C). In Sec. II we describe our experimental results in PrInAg₂, which include the temperature dependence of the zero-field μ^+ relaxation and the longitudinal field dependence of the relaxation at selected temperatures. The implications of these results for the nature of the low-temperature state of PrInAg₂ are discussed in Sec. III, where we also argue that the effect of the μ^+ electric charge on its environment does not invalidate our analysis. We summarize our results in Sec. IV.

A. Nonmagnetic Kondo effect

To our knowledge the only nonmagnetic mechanism for Kondo behavior proposed to date is the two-channel quadrupolar Kondo effect (QKE) of Cox.⁵ In this picture, which was developed to explain the unexpected lack of field dependence of heavy-fermion properties in uranium-based compounds, correlated-electron behavior occurs when a non-Kramers f ion such as Pr³⁺ possesses a nonmagnetic multiplet ground state. The fluctuating electric quadrupole moment of the ground state scatters conduction electrons, analogous to spin-fluctuation scattering in the usual Kondo effect. An important difference between the two effects is that in the QKE there are two conduction-electron channels (spin-up and spin-down); since spin plays no role in the nonmagnetic scattering, the spin directions serve only as labels. The QKE is therefore one of a class of *multichannel* Kondo effects^{6,7} for which the low-temperature behavior is that of a ‘‘non-Fermi-liquid’’ with unusual properties, e.g., logarithmic divergence of $\gamma(T)$ and nonzero residual entropy $S(T=0) = \frac{1}{2}R \ln 2$.

In its original form the theory of the QKE considers isolated impurities only, and to our knowledge no treatment of a lattice of nonmagnetic QKE f ions has appeared. In particular, it is apparently not known whether the non-Fermi-liquid behavior of the impurity problem survives in the lattice. Although Yatskar *et al.*¹ observed an uncharacteristic temperature dependence of the low-temperature electrical resistivity in PrInAg₂, they found a substantially temperature-independent $\gamma(T)$ below ~ 0.2 K and no evidence for residual entropy. Thus it is unclear whether or not PrInAg₂ is a Fermi liquid.

B. Zero- and longitudinal-field muon spin relaxation

μ SR is a sensitive local probe of static and dynamic magnetism in solids.⁸ Spin-polarized positive muons are implanted into the sample, and the subsequent decay of the μ^+ spin polarization is monitored in time by measuring the asymmetry in the numbers of decay positrons emitted parallel and antiparallel to the μ^+ spin direction. The resulting relaxation function $G(t)$ is analogous to the free induction signal in a pulsed nuclear magnetic resonance (NMR) experiment. It is straightforward to carry out μ SR experiments in zero or weak applied magnetic fields, which is not the case for NMR.

The shape and duration of $G(t)$ are controlled by the local magnetic fields at the muon sites due to their magnetic environments. There are two kinds of effects. Relaxation by *static* local fields reflects a spatial distribution of μ^+ Larmor precession frequencies and hence of the local fields. The decay of $G(t)$ is then due to loss of phase coherence between precessing μ^+ spins, and the relaxation time is of the order of the inverse of the spread in Larmor frequencies. If the μ^+ local field distribution is due to randomly oriented neighboring magnetic dipole moments (nuclear or electronic), the Central Limit Theorem suggests a Gaussian field distribution if more than a few moments contribute, in which case $G(t)$ is also Gaussian. Fields due to randomly oriented nuclear dipolar moments, which usually do not reorient on the time scale of μ SR experiments,⁹ often give rise to static relaxation. μ SR is also a very good test for static magnetism, with or without long-range order, with a sensitivity $\sim 10^{-3} \mu_B$, since dipolar fields from such small moments produce observable static relaxation. *Dynamic* (fluctuating) μ^+ local fields lead to spin-lattice relaxation, as in NMR, which is a measure of the spectral density of the fluctuations at low frequencies. For dynamic relaxation $G(t)$ is often but not always exponential.

Static and dynamic relaxation mechanisms can be distinguished by μ SR experiments in a longitudinal magnetic field \mathbf{H}_L (i.e., a field parallel to the μ^+ spin direction) much larger in magnitude than a typical local field \mathbf{H}_{loc} . This produces a resultant field $\mathbf{H}_L + \mathbf{H}_{\text{loc}}$ essentially in the direction of the applied field and hence of the μ^+ spin. Then the muons do not precess substantially, and if \mathbf{H}_{loc} is static their spin polarization is maintained indefinitely. This procedure is known as ‘‘decoupling’’ of the μ^+ spin from the static local fields. If, on the other hand, the relaxation is dynamic, then it is usually much less affected by the relatively weak applied field (typically $H_L \lesssim 100$ Oe). The expected field for decoupling is a few times the spread ΔH_{loc} in local fields, which can be estimated self-consistently by assuming that the relaxation is static. In this case the observed relaxation rate gives the spread σ of μ^+ precession frequencies, so that

$$\Delta H_{\text{loc}} = \sigma / \gamma_\mu, \quad (1)$$

where γ_μ is the μ^+ gyromagnetic ratio.

Zero-field and longitudinal-field μ SR (ZF- and LF- μ SR) relaxation data are often analyzed using the Kubo-Toyabe (K-T) model,¹⁰ which treats the distribution and dynamical fluctuation of \mathbf{H}_{loc} . This model determines the shape of the relaxation function and its rate of decay as a function of H_L and the parameters that characterize \mathbf{H}_{loc} . Details of the K-T model and its application will be discussed below in Sec. II A.

C. Hyperfine-enhanced nuclear magnetism

The best-known hyperfine-enhancement effect is the enhancement of the applied field at the nuclear site by a factor $1 + K$ (Ref. 3), with

$$K = a_{\text{hf}} \chi_{\text{VV}}. \quad (2)$$

Here a_{hf} is the f atomic hyperfine coupling constant, expressed in units of mole emu⁻¹, and χ_{VV} is the (molar) Van

Vleck susceptibility of the f ions. The factor K is the usual paramagnetic NMR frequency shift (Knight shift in metals), due in this case to χ_{VV} . The latter is given approximately by

$$\chi_{VV} \approx \frac{C}{(\Delta_{\text{CEF}}/k_B)}, \quad (3)$$

where C is the f -ion Curie constant and Δ_{CEF} is the excitation energy of the lowest CEF magnetic excited state. For typical Pr^{3+} splittings $\Delta_{\text{CEF}}=10\text{--}100$ K, so that $\chi_{VV}=0.01\text{--}0.1$ emu mole $^{-1}$. With $a_{\text{hf}}(\text{Pr}^{3+})=187.7$ mole emu $^{-1}$ (Ref. 11), one finds $K=2\text{--}20$. These considerable field increases are used to attain very low temperatures by nuclear demagnetization of singlet-ground-state Pr-based intermetallics.^{12,13}

Other effects of hyperfine enhancement include the following:¹⁴

(i) The f electrons are polarized by the nuclear magnetic dipole moment via a Van Vleck-like response, leading to an enhanced effective nuclear moment $\mu_{\text{nuc}}^{(\text{enh})}=(1+K)\mu_{\text{nuc}}^{(\text{bare})}$. The nuclear moment itself is of course unchanged; the term ‘‘hyperfine enhancement,’’ used here in much the same sense as ‘‘many-body enhancement of the electron mass’’ in heavy-fermion systems, refers to the interaction of the effective (nuclear+ f -electron) moment with its magnetic environment.

(ii) The electronic exchange coupling between neighboring f ions mediates an indirect exchange interaction between nuclear spins, with exchange constant \mathcal{J}_{nuc} given by

$$\mathcal{J}_{\text{nuc}} = \left(\frac{\gamma_{\text{nuc}} \hbar}{g_J \mu_B} \right)^2 K^2 \mathcal{J}_{\text{el}}; \quad (4)$$

here γ_{nuc} is the nuclear gyromagnetic moment and \mathcal{J}_{el} is the electronic exchange constant.

Bleaney¹⁴ describes this situation as ‘‘. . . dealing with nuclear lambs in electronic wolves’ clothing.’’

Hyperfine enhancement phenomena were first observed in singlet ground-state f -ion compounds, but are also expected for f ions with nonmagnetic multiplet ground states. Such effects do not occur at temperatures $\geq \Delta_{\text{CEF}}/k_B$ (Ref. 4) or if the ground state of the f ion is magnetic. In both of these circumstances the f -electron polarization induced by the nucleus is lost in the much larger electronic magnetic moment of the f ion, and hyperfine-enhancement phenomena are obliterated.

II. EXPERIMENTAL RESULTS

The powdered sample of PrInAg_2 was prepared as described previously.¹ μSR experiments were carried out at the πM3 beam line of the Paul Scherrer Institute (PSI), Villigen, Switzerland, using the General Purpose Spectrometer (GPS) and Low Temperature Facility (LTF), and at the M20 beam line at TRIUMF, Vancouver, Canada. ZF- μSR data were obtained over the temperature range 0.1–100 K. The dependence of the relaxation function on longitudinal field was also studied at a number of temperatures in this range. We describe these results below, and discuss their implications in Sec. III.

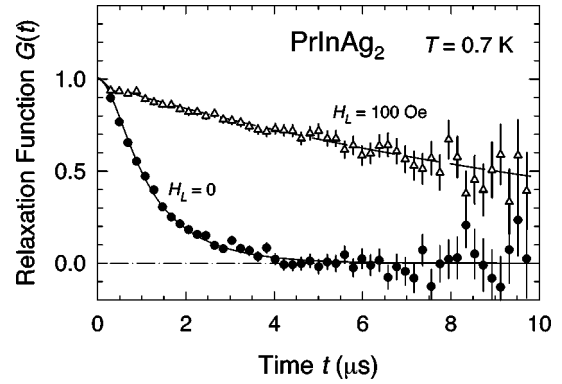


FIG. 1. μ^+ relaxation function $G(t)$ in PrInAg_2 , $T=0.7$ K. The relaxation for longitudinal applied field $H_L=100$ Oe (triangles) is much faster than expected if the zero-field relaxation (circles) were due to a static distribution of local fields. Curves: fits to dynamic K-T model (Refs. 10 and 15) for $H_L=0$ (solid curve) and $H_L=100$ Oe (dashed curve).

A. ZF and LF muon relaxation

We use the K-T model^{10,15} to analyze μ^+ relaxation in zero and longitudinal applied fields at selected temperatures between 0.7 K and 100 K. The K-T model assumes that the local field \mathbf{H}_{loc} is distributed in magnitude and direction, with each Cartesian component distributed around zero with rms value σ/γ_μ , and that \mathbf{H}_{loc} fluctuates randomly in time with fluctuation rate ν . Henceforth we refer to σ as the static relaxation rate, because it characterizes the μ^+ relaxation in the ‘‘static’’ K-T model in the absence of fluctuations ($\nu=0$). We treat the K-T model in the ‘‘strong-collision’’ approximation of Hayano *et al.*,¹⁵ which takes the fluctuation to be of the form of sudden uncorrelated jumps of \mathbf{H}_{loc} .¹⁶

Figure 1 shows experimental μ^+ relaxation functions $G(t)$ in PrInAg_2 for $T=0.7$ K in zero field and in a longitudinal applied field $H_L=100$ Oe. If the relaxation were due to a distribution of static μ^+ local fields, the observed ZF relaxation rate leads to an estimate of ~ 10 Oe for the spread of these local fields. Then a longitudinal field of 100 Oe should completely decouple the local fields and there should be no relaxation. But it can be seen from Fig. 1 that although the relaxation rate is reduced for $H_L=100$ Oe it remains appreciable ($\sim 0.07 \mu\text{s}^{-1}$). This strongly suggests that dynamic relaxation is involved.

The curves in Fig. 1 are the results of simultaneous fits of the ZF and LF data to the dynamic K-T model of μ^+ relaxation.^{10,15} The best-fit parameters from this and subsequent fits are given in Table I.

ZF and LF relaxation data at temperatures of 10 K and 30 K are given in Fig. 2. As could be anticipated from the discussion of Sec. II A, the relaxation function $G(t)$ at 10 K closely resembles $G(t)$ at 0.7 K (Fig. 1). By 30 K, however, the overall relaxation rate in zero field has decreased substantially, and a longitudinal field of 200 Oe rather than 100 Oe is required to increase $G(t=10\mu\text{s})$ to ~ 0.5 (cf. Fig. 1). In Fig. 2 as in Fig. 1 the curves are fits to the dynamic K-T model; the fit values of σ and ν are given in Table I.

Figure 3 shows relaxation data at 100 K for $H_L=0, 20,$ and 50 Oe. Here the situation is very different than for $T \lesssim 30$ K. A longitudinal field of 20 Oe is sufficient to reduce the overall relaxation rate significantly; the rate in 20 Oe and

TABLE I. Relaxation parameters from fits of ZF and LF μ^+ relaxation data to dynamic and damped static K-T models (Refs. 10 and 15) for selected temperatures T and applied longitudinal fields H_L . σ : Static relaxation rate (local-field distribution width in frequency units). ν : local-field fluctuation rate in dynamic K-T model. R : dynamic relaxation rate in damped static K-T model. The dynamic K-T model fits the data well up to 30 K. At 100 K the data are well fit by the damped static K-T function [Fig. 3(b)], whereas a dynamic K-T fit is not justified by the field dependence of the relaxation function [Fig. 3(a)].

T (K)	H_L (Oe)	σ (μs^{-1})	ν (μs^{-1})	R (μs^{-1})
0.7	0,100	1.15 ± 0.05	2.2 ± 0.1	
10	0,100	1.20 ± 0.05	2.85 ± 0.1	
30	0,200	1.20 ± 0.05	9.0 ± 0.5	
100	0, 50	0.28 ± 0.02	0.7 ± 0.1	
100	0, 50	0.15 ± 0.02		0.04 ± 0.01

greater, while nonzero, is not affected by further increase of H_L . This is much closer to the decoupling behavior expected for static broadening, as discussed in Sec. I B.

The curves in Fig. 3(a) show the results of a dynamic K-T fit to the ZF and 50-Oe data, for which values of σ and ν are also given in Table I. There are two difficulties with the results of this fit. First, the values of σ and ν deviate appreciably from the trend established by the results for $T \leq 30$ K (cf. Table I). Second, and more compelling, the best-fit values for $H_L=0$ and 50 Oe yield a predicted dynamic K-T $G(t)$ for $H_L=20$ Oe that lies considerably below the data. A dynamic K-T fit to the ZF and 20-Oe data (not shown) is no more successful, because then the predicted $G(t)$ for $H_L=50$ Oe lies considerably above the data.

These results indicate that at 100 K the dynamic K-T model is no longer applicable, i.e., the dynamic behavior of H_L is not simply represented by a single static relaxation rate σ and fluctuation rate ν . Instead, it appears that the nuclear dipole contribution to H_L is static or nearly so at this temperature, so that it is decoupled for $H_L \geq 20$ Oe. The appre-

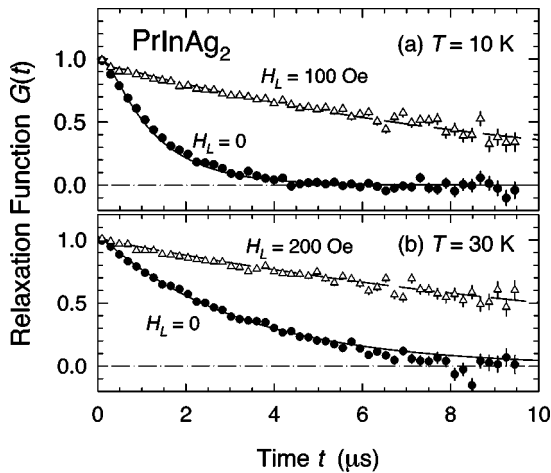


FIG. 2. Dependence of μ^+ relaxation function $G(t)$ on longitudinal applied field H_L in PrInAg₂. (a) $T=10$ K. The data are similar to those at 0.7 K (Fig. 1). (b) $T=30$ K. Here the ZF data manifest a reduction of the μ^+ relaxation rate. Curves: fits to the dynamic K-T model.

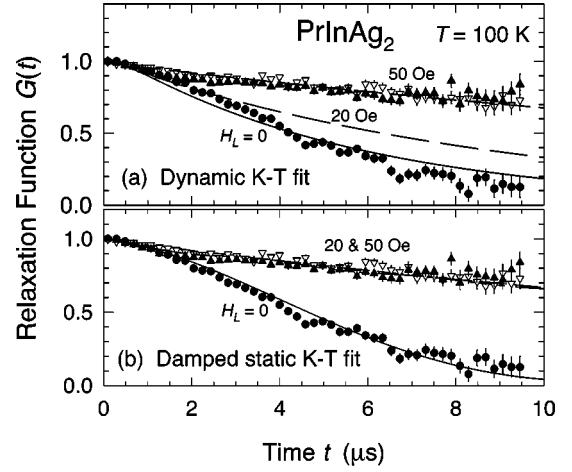


FIG. 3. (a) Dependence of μ^+ relaxation function $G(t)$ on longitudinal applied field H_L in PrInAg₂, $T=100$ K. Circles: zero field. Open triangles: $H_L=20$ Oe. Filled triangles: $H_L=50$ Oe. The data are independent of field for $H_L \geq 20$ Oe. Solid curves: Fits of dynamic K-T model to data for $H_L=0$ and 50 Oe. Dashed curve: prediction of dynamic K-T model for $H_L=20$ Oe. (b) Same data; fits to damped static K-T model given by $G(t)=G_0(T)\exp(-Rt)$. Curves: fits for $H_L=0$, 20 Oe, and 50 Oe. (The latter two are indistinguishable.) The damped static K-T fits reproduce the form and field dependence of the data much better than the dynamic K-T fits.

ciable relaxation observed in these fields must then be due to a second contribution to H_L , for which the obvious candidate is a fluctuating transferred hyperfine coupling to thermally excited Pr^{3+} moments. Such a process would also contribute to the relaxation in zero field. This situation can be modeled using the “damped static” K-T function

$$G(H_L, t) = G_0(H_L, T) \exp(-Rt), \quad (5)$$

where $G_0(H_L, t)$ is the static K-T function at longitudinal field H_L and R is the dynamic relaxation rate due to the fluctuating component of H_L . Fits to this function are shown in Fig. 3(b), where it can be seen that the form and field dependence of $G(t)$ are far better reproduced than in Fig. 3(a). The situation is reminiscent of the nuclear-electronic double relaxation behavior found in rare-earth rhodium borides by Noakes *et al.*¹⁷ and in MnSi by Matsuzaki *et al.*,¹⁸ except that here the ground state is nonmagnetic and the local moment corresponds to thermally populated CEF states.

Values of σ , ν , and R for dynamic K-T fits [σ and ν , Figs. 1–3(a)] and damped static K-T fits [σ and R , Eq. (5), Fig. 3(b)] are given in Table I. At 0.7 K $\nu \approx 1.9\sigma$, so that the relaxation is in the regime of moderate motional narrowing. The fits indicate little change of σ but an increase of ν with increasing temperature up to 30 K. Finally, at 100 K the damped static K-T fit shows a marked reduction of σ compared to its value at and below 30 K. We defer detailed discussion of these results to Sec. III B.

B. ZF muon relaxation between 0.1 K and 100 K

In zero field a crossover occurs with increasing fluctuation rate from the “quasistatic” regime ($\nu \ll \sigma$) to the “motion-

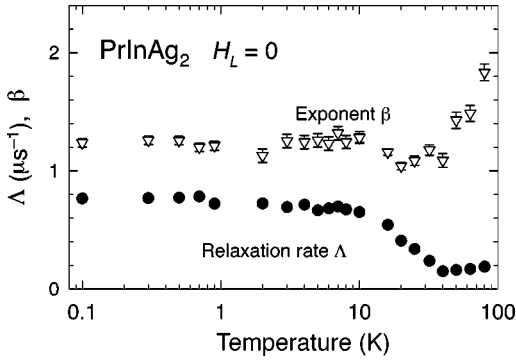


FIG. 4. Temperature dependence of the zero-field μ^+ relaxation rate Λ (circles) and exponent β (triangles) in PrInAg_2 from fits of a ‘‘power exponential’’ function $G(t) = \exp[-(\Lambda t)^\beta]$ to ZF- μ SR relaxation data.

ally narrowed’’ regime ($\nu \gg \sigma$). For $\nu \gtrsim \sigma$ the main dependence of the ZF relaxation function is on the combination σ^2/ν ; the dependence on σ and ν separately is weaker (and vanishes in the motionally narrowed limit). Thus for moderate to extreme motional narrowing the ZF data alone do not suffice to determine both parameters, and the added constraint provided by the data in applied field is essential.

The combined ZF and LF relaxation data of Sec. II A characterize the muon relaxation at several discrete temperatures between 0.7 K and 100 K. Only ZF data are available for other temperatures, and fits to dynamic K-T relaxation functions are not useful. The data can, however, be roughly parameterized by fitting to a ‘‘power exponential’’ function

$$G(t) = \exp[-(\Lambda t)^\beta], \quad (6)$$

where Λ is a generalized relaxation rate and the exponent β interpolates between exponential ($\beta=1$) and Gaussian ($\beta=2$) limits. This fit function has no physical justification, but its parameters give a crude indication of the behavior of the relaxation, i.e., whether as discussed in Sec. I B it is dynamic (exponential), static (Gaussian), or an intermediate case. The value and temperature dependence of the rate Λ also gives additional qualitative information on the origin of \mathbf{H}_{loc} and the behavior of its thermal fluctuations. This approach is similar to that of Crook and Cywinski,¹⁹ who showed that a ‘‘power Kubo-Toyabe’’ function characterizes the case where the local field distribution is a superposition of independent Gaussian and Lorentzian components. We do not use the results of Crook and Cywinski, however, as there is no evidence from our ZF/LF data for such a mixed distribution.

The parameters Λ and β are plotted versus temperature in Fig. 4. Both parameters are essentially independent of temperature from 0.1 K to ~ 10 K. There is, therefore, no sign in this temperature range of the temperature-dependent relaxation expected from either of two mechanisms: (a) the onset of static magnetism with decreasing temperature due to either ordered or spin-glass-like spin freezing, or (b) thermal fluctuations of conventional (spin) Kondo ions. The low-temperature value $\beta \approx 1.2$ indicates that the relaxation is nearly but not quite exponential, consistent with the dynamic K-T model in the moderately motionally narrowed regime. We consider these results in more detail in Sec. III A below.

Above 10 K both Λ and β vary with temperature. A decrease of Λ to $0.18 \mu\text{s}^{-1}$ occurs between ~ 10 K and ~ 50 K, and above 50 K β increases to ~ 2 at 80 K. In the K-T model this suggests an increase of the fluctuation rate ν with increasing temperature, followed by a crossover to static or nearly static relaxation at high temperatures. This is qualitatively the picture obtained from our LF decoupling experiments as described in Sec. II A.

III. DISCUSSION

We first consider the implications of the temperature independence of the ZF relaxation between 0.1 K and ~ 10 K, using the rough ‘‘power exponential’’ analysis of Sec. II B and the data of Fig. 4. We argue that the data are incompatible with explanations of the specific-heat anomaly that invoke a magnetic Pr^{3+} ground state.

We then discuss the results of our K-T analyses of the data of Figs. 1–3. We show that (a) the temperature and field dependence of the relaxation between 0.1 K and 100 K is quantitatively explained by nuclear dipole coupling alone (including ^{141}Pr hyperfine enhancement at low temperatures), (b) little or no Pr^{3+} electronic paramagnetism need be invoked in the temperature range 0.1–10 K, and (c) the ^{141}Pr nuclear-spin fluctuation rate in this range is consistent with the indirect nuclear exchange mechanism described above in Sec. I C.

Finally, we consider (and reject) the possibility that this nonmagnetic or weak-moment state is due to Kondo compensation with a high characteristic temperature, and also the possibility that perturbation of the Pr^{3+} CEF scheme by the μ^+ electric charge leads to the observed μ^+ relaxation phenomena.

A. Zero-field muon relaxation rate at low temperatures

The data of Fig. 4 put an upper bound of $\sim 0.05 \mu\text{s}^{-1}$ on any change of Λ between 0.1 K and ~ 10 K. This result has important implications for alternative explanations of the low-temperature specific-heat anomaly of Yatskar *et al.*¹ that involve hypothetical Pr^{3+} magnetic moments: (a) weak-moment static magnetism due to spin freezing, (b) ‘‘conventional’’ Kondo spin fluctuations characterized by a Kondo temperature $T_K \sim 1$ K, and (c) geometric frustration of Pr^{3+} magnetic ordering.

The effect of such Pr^{3+} moments on muon relaxation is described in the K-T model by the static relaxation rate σ and the fluctuation rate ν . We have seen above that a K-T analysis leads to the same value of σ at 0.7 K and 10 K (and even at 30 K) within experimental error. The temperature independence of both Λ and β between 0.1 K and 10 K (Fig. 4) strongly suggests that the functional form of $G(t)$ and hence σ and ν are nearly constant over this range of temperatures. In the following we treat $\Lambda(T)$ as if it were either a static μ^+ relaxation rate (i.e., σ) or a dynamic μ^+ relaxation rate (i.e., $\approx 2\sigma^2/\nu$ in the motionally narrowed limit), depending on the hypothetical situation, and consider the effect of the experimental upper bound of $\sim 0.05 \mu\text{s}^{-1}$ on any temperature dependence of Λ (Fig. 4).

a. Weak-moment static magnetism. Spin freezing and the onset of static magnetism (ordered or disordered) below

0.5–1 K would be expected to produce an increase of the static relaxation rate below the freezing temperature T_f . Thus the temperature-independent relaxation rate observed between 0.1 K and 10 K (Fig. 4) cannot be understood in terms of such spin freezing. We nevertheless take the observed relaxation rate $\Lambda(T)$ to be primarily due to a temperature-independent rate Λ_0 , of unknown origin, and examine the consequences of an additional temperature-dependent static rate $\delta\lambda(T)$ due to spin freezing. We assume conservatively that Λ_0 and $\delta\lambda(T)$ add in quadrature, with $\Lambda_0 \approx 0.8 \mu\text{s}^{-1}$. Then with $\Lambda(T) - \Lambda_0 \leq 0.05 \mu\text{s}^{-1}$ we have

$$\delta\lambda \approx \sqrt{2\Lambda_0[\Lambda(T) - \Lambda_0]} \leq 0.3 \mu\text{s}^{-1}. \quad (7)$$

Equivalently, an upper bound on the static μ^+ local field H_f due to spin freezing is given by

$$H_f = \delta\lambda / \gamma_\mu \leq 3 \text{ Oe}. \quad (8)$$

We relate this result to the hypothetical frozen Pr^{3+} magnetic moment μ_f using the ratio $H_{\text{loc}} / \mu_f \sim 1 \text{ kOe} / \mu_B$ calculated from a lattice sum over Pr sites. This yields an upper bound on μ_f of order

$$\mu_f \leq 3 \times 10^{-3} \mu_B. \quad (9)$$

Static magnetism is therefore ruled out at this level. If Λ_0 and $\delta\lambda$ were assumed to add linearly the upper limits on $\delta\lambda$ and μ_f would be much smaller: $\delta\lambda \leq 0.05 \mu\text{s}^{-1}$ and $\mu_f \leq 5 \times 10^{-4} \mu_B$, respectively.

Pr^{3+} spin freezing with such weak frozen moments could, of course, still occur. But in general weak moments are associated with a Kondo temperature T_K , which is high compared to T_f . Then Kondo compensation removes most of the spin entropy at temperatures $\sim T_K$, leaving only a weak specific-heat anomaly at T_f .²⁰ Thus the large entropy developed below 1 K (Ref. 1) is unlikely to be associated with weak-moment spin freezing, which also leaves unexplained the strong and essentially temperature-independent μ^+ relaxation in the range 0.1–10 K. We conclude that spin freezing is not the origin of the low-temperature Kondo behavior, leaving to Sec. III C the question of whether weak-moment paramagnetism may play a role in the hyperfine-enhanced behavior of PrInAg_2 .

It should be noted that these results are not sensitive to the use of crude power-exponential fits rather than the more appropriate dynamic K-T analysis. The K-T value of σ is about 40% greater than Λ_0 , so that use of it in the above analysis would increase the experimental upper bound on any frozen Pr^{3+} moment by $\sim 20\%$ [cf. Eq. (7)]. This does not change our conclusion that spin freezing is not responsible for the 0.5-K specific-heat anomaly.

b. Conventional (spin) Kondo physics. Yatskar *et al.*¹ ruled out a conventional Kondo effect with $T_K \sim 1 \text{ K}$, noting that inelastic neutron-scattering experiments² indicated a nonmagnetic Γ_3 doublet Pr^{3+} CEF-split ground state. We nevertheless consider the possibility that the 0.5-K specific-heat feature is a conventional Kondo anomaly, i.e., that it is magnetic in origin.

For temperatures $\leq T_K$, a Kondo spin fluctuates at a rate $\nu_K \approx k_B T_K / \hbar$, which is $\sim 10^{11} \text{ s}^{-1}$ for $T_K \approx 1 \text{ K}$. In the neighborhood of T_K the μ^+ relaxation rate T_1^{-1} is a maximum given by

$$(T_1^{-1})_{\text{max}} \approx 2\sigma^2 / \nu_K; \quad (10)$$

here $\sigma \approx \gamma_\mu H_{\text{loc}}$ is the μ^+ / Pr^{3+} dipole coupling in frequency units. We estimate σ using the value $H_{\text{loc}} = 1.10 \text{ kOe} / \mu_B$ calculated from a lattice sum over Pr sites assuming uncorrelated Pr-moment fluctuations. This gives

$$(T_1^{-1})_{\text{max}} \approx 0.2 \mu\text{s}^{-1} \quad (11)$$

for an uncompensated Pr^{3+} moment of the order of 1 μ_B . We expect this rate for $T \geq T_K$, with a crossover to a Korringa law

$$T_1^{-1} \approx (T_1^{-1})_{\text{max}} \left(\frac{T}{T_K} \right) \quad (12)$$

(i.e., a considerable decrease of T_1^{-1}) for $T < T_K$.

To compare this scenario with the experimental results we assume that $\Lambda(T)$ is dynamic in origin, i.e., $\Lambda \approx T_1^{-1}$. We see that the observed rate $\Lambda \approx 0.8 \mu\text{s}^{-1}$ is constant down to $\sim 0.1 \text{ K}$ (Fig. 4), whereas from Eq. (12) and $T_K \approx 1 \text{ K}$ (Ref. 1) one expects a decrease of T_1^{-1} at 0.1 K to $\sim 10\%$ of its value at 1 K. It might be argued that the Korringa rate is masked by a temperature-independent rate Λ_0 , as in the discussion of spin freezing, in which case the minimum observable change of $0.3\text{--}0.4 \mu\text{s}^{-1}$ derived above would apply and a Korringa-like change of $\sim 0.2 \mu\text{s}^{-1}$ could not be ruled out by the data. But in the conventional Kondo scenario, as in the spin-freezing picture, there is no mechanism for a temperature-independent rate as large as Λ_0 . We therefore conclude that the experimental results are not consistent with conventional Kondo behavior.

c. Frustrated coupling between Pr^{3+} moments. In certain lattices, including the fcc lattice of PrInAg_2 , Néel magnetic ordering due to nearest-neighbor couplings can be precluded by the lattice symmetry, a situation known generally as frustration of the ordering.²¹ In a recent study of the frustrated pyrochlore antiferromagnet $\text{Tb}_2\text{Ti}_2\text{O}_7$,²² in which there was no sign of ordering, the zero-field muon relaxation rate was found to increase with decreasing temperature down to $\sim 1 \text{ K}$ and then remain constant at a value of $\sim 2.5 \mu\text{s}^{-1}$ down to 70 mK. This is the same sort of behavior exhibited by $\Lambda(T)$ in Fig. 4. Frustrated ordering cannot be occurring in PrInAg_2 , however, since the dynamic K-T analyses at 0.7 K and 10 K indicate $\Delta H_{\text{loc}} = \sigma / \gamma_\mu \approx 10 \text{ Oe}$; this is two orders of magnitude smaller than the dipolar coupling to Pr^{3+} moments $\sim 1 \mu_B$.

B. Nuclear magnetism and muon relaxation

In this section we argue that the results of Sec. II can be understood by assuming that (1) nuclear magnetism is the principal source of the μ^+ local field \mathbf{H}_{loc} , and (2) the ^{141}Pr nuclear magnetism is hyperfine enhanced at low temperatures. Both of these conclusions are necessary consequences of the hypothesis of a nonmagnetic CEF-split ground state.

We first consider the μ^+ relaxation behavior for temperatures up to $\sim 30 \text{ K}$. The decrease of the power-exponential relaxation rate $\Lambda(T)$ above $\sim 10 \text{ K}$ (Fig. 4) suggests the onset of ^{141}Pr nuclear spin-lattice relaxation by thermally-populated magnetic Pr^{3+} CEF excited states; the corresponding increase of the fluctuation rate ν ‘‘otionally narrows’’

the μ^+ relaxation rate. This picture is confirmed by the data of Figs. 1–3, since as shown in Table I the data suggest a temperature-independent static rate σ and steadily increasing $\nu(T)$.

At sufficiently high temperatures (above $\Delta_{\text{CEF}}/k_B \approx 60$ K) the exponent β (Fig. 4) tends to the value $\beta=2$ characteristic of a Gaussian relaxation rate, reflecting the Gaussian short-time behavior of the static K-T relaxation function.¹⁰ At the same time the relaxation rate tends to a value $\sim 0.2 \mu\text{s}^{-1}$, characteristic of μ^+ relaxation by static (and unenhanced) nuclear moments.

Two possibilities for this high-temperature nuclear relaxation suggest themselves. The ^{141}Pr relaxation may remain so rapid that the contribution of ^{141}Pr dipolar fields to the μ^+ local field is motionally narrowed, and only the ^{115}In nuclei contribute significantly. Alternatively, the Pr^{3+} fluctuations could become fast enough so that their contribution to the ^{141}Pr relaxation itself becomes motionally narrowed and negligible. Then the ^{141}Pr nuclei would relax under the influence of both (unenhanced) ^{141}Pr and ^{115}In nuclear dipolar fields.

We shall see that our results suggest the former possibility. In either event the μ^+ relaxation at high temperatures (~ 100 K) is describable by the K-T model in the quasi-static limit, possibly with dynamic relaxation due to thermally excited Pr^{3+} spin fluctuations. Such a picture is supported by the results of Fig. 3, since the ZF relaxation is easily decoupled by a longitudinal field of 20 Oe ($H_L \gg \sigma/\gamma_\mu \approx 1.2$ Oe).

The above scenario can be put on a more quantitative footing by comparing the data with the expected relaxation behavior at low and high temperatures, i.e., with and without hyperfine enhancement, respectively. We start by determining the expected nuclear relaxation at high temperatures, where one has static dipolar broadening from ^{115}In nuclei, together with a contribution from (unenhanced) ^{141}Pr nuclei if this latter contribution is not motionally narrowed. These nuclear contributions to the μ^+ relaxation can be calculated using the usual Van Vleck method of moments.²³

The μ^+ electric charge produces an electric-field gradient at the ^{141}Pr ($I=5/2$) and ^{115}In ($I=9/2$) sites. This produces a quadrupole splitting for both nuclides, which are not split in the unperturbed crystal because both sites possess cubic point symmetry. The quadrupole splitting in turn modifies the secular terms in the dipolar interaction, which must be taken into account in calculating the μ^+ relaxation in zero field.^{15,24} The μ^+ stopping site is unknown in PrInAg_2 . Calculated values of σ for candidate μ^+ sites are shown in Table II, which gives individual contributions $^{141}\sigma_{\text{ZF}}$ and $^{115}\sigma_{\text{ZF}}$ from ^{141}Pr and ^{115}In nuclei, respectively, together with the total rate $\sigma_{\text{ZF}}^{\text{tot}} = (^{141}\sigma_{\text{ZF}}^2 + ^{115}\sigma_{\text{ZF}}^2)^{1/2}$. Best agreement with the observed high-temperature static rate is found for the $(\frac{1}{4}, \frac{1}{4}, 0)d$ site (Wyckoff notation) with a contribution to $\sigma_{\text{ZF}}^{\text{tot}}$ from ^{115}In nuclei but not from ^{141}Pr nuclei. This is consistent with the first of the two hypotheses discussed above.

The μ^+ charge may distort the lattice locally, thereby modifying the near-neighbor dipolar interactions primarily responsible for the relaxation. These dipolar interactions vary as the cube of the near-neighbor distances, the change

TABLE II. Calculated powder-average ZF- μ SR static Gaussian relaxation rates σ_{ZF} for candidate μ^+ sites in PrInAg_2 , assuming quadrupole splitting by the μ^+ electric field gradient (Refs. 15 and 24). Individual contributions $^{141}\sigma_{\text{ZF}}$ and $^{115}\sigma_{\text{ZF}}$ from ^{141}Pr and ^{115}In nuclei, respectively, are shown, together with the total rate $\sigma_{\text{ZF}}^{\text{tot}}$. The observed high-temperature rate (Table I) is given for comparison.

Site (Wyckoff notation)	Coordinates	$^{141}\sigma_{\text{ZF}}$ (μs^{-1})	$^{115}\sigma_{\text{ZF}}$ (μs^{-1})	$\sigma_{\text{ZF}}^{\text{tot}}$ (μs^{-1})
<i>d</i>	$(\frac{1}{4}, \frac{1}{4}, 0)$	0.1329	0.1667	0.2132
<i>e</i>	$(\frac{1}{4}, 0, 0)$	0.2570	0.3227	0.4125
<i>f</i>	$(\frac{1}{8}, \frac{1}{8}, \frac{1}{8})$	0.3906	0.1286	0.4113
Observed				0.15 ± 0.02

of which can therefore be estimated from a comparison of calculated and measured μ^+ static relaxation rates. This yields a local dilatation of $3 \pm 2\%$, assuming the muon occupies the *d* site and that only the ^{115}In contribution is present. This is comparable to the values 2–5% found in copper under similar circumstances by Camani *et al.*²⁵ and Luke *et al.*,²⁶ but the high-temperature data are equally consistent with little if any dilatation.

At low temperatures the ^{141}Pr contribution to the μ^+ static relaxation rate is increased by a factor $1+K$ if the ^{141}Pr dipole moment is hyperfine enhanced (Sec. I C). Using $a_{\text{hf}} = 187.7$ mole emu⁻¹ (Ref. 11) and the extrapolated low-temperature Van Vleck susceptibility $\chi_{\text{VV}}(0) \approx 0.040$ emu mole⁻¹ (Ref. 1), we obtain $K \approx 7.5$ from Eq. (2), in agreement with the value obtained from the nuclear Schottky anomaly in the low-temperature specific heat.²⁷ This gives an expected low-temperature rate

$$\sigma(\text{low } T) = [^{141}\sigma_{\text{ZF}}^2(1+K)^2 + ^{115}\sigma_{\text{ZF}}^2]^{1/2} = 1.14 \mu\text{s}^{-1}$$

for the *d* site, in excellent agreement with the observed low-temperature value of $1.15 \pm 0.05 \mu\text{s}^{-1}$ quoted above.

We now turn to the observed value $\nu = 2.2 \mu\text{s}^{-1}$ of the low-temperature fluctuation rate (Table I). The magnitude and temperature independence of this rate below 10 K lead us to interpret it as due to the like-spin coupling between (hyperfine-enhanced) ^{141}Pr nuclear moments. Using the Van Vleck method of moments, the calculated ^{141}Pr zero-field rms relaxation rate (neglecting quadrupolar splitting) is $^{141}\sigma_{\text{ZF}} = 0.7490 \mu\text{s}^{-1}$. This is smaller than the observed fluctuation rate by a factor of ~ 3 .

We first attempt to resolve this discrepancy by noting that the electric-field gradient due to the μ^+ charge will induce quadrupole splitting of the neighboring ^{141}Pr nuclei. The effect of this splitting on the μ^+ spin dynamics has been taken into account, but it also has an effect on the ^{141}Pr relaxation. In the presence of such quadrupole splitting the like-spin zero-field linewidth has only been calculated for $I=1$ and $3/2$ (Ref. 23), where it is found that σ_{ZF} is increased by factors of 1.19 and 1.26, respectively. These are not enough to explain the shortfall. It is likely that the corresponding factor for $I=5/2$ is larger than 1.26, but the trend does not seem to allow explanation of a factor of 3 by this mechanism.

We next consider the indirect exchange interaction between ^{141}Pr nuclei described in Sec. I C, which is mediated by the electronic exchange between neighboring Pr^{3+} ions. We take the observed fluctuation rate ν as a measure of the nuclear exchange constant $\mathcal{J}_{\text{nuc}}/\hbar$, and use $K=7.5$ and Eq. (4) to obtain the estimate

$$\mathcal{J}_{\text{el}}/k_B \approx 0.19 \text{ K} \quad (13)$$

for the electronic exchange constant \mathcal{J}_{el} . This is comparable to results in other nonmagnetic-ground-state Pr-based compounds: $\mathcal{J}_{\text{el}}/k_B=0.61$ K in PrP (Ref. 28) and 0.39 K in PrNi₅ (Ref. 29). In PrInAg₂ $\mathcal{J}_{\text{el}}/k_B$ is of the same order as the Kondo temperature scale of 0.5–1 K, and may therefore play a role in the theory of the nonmagnetic Kondo effect in this system.

C. Weak-moment paramagnetism?

The Pr^{3+} ground state would also be “nonmagnetic” if the Pr^{3+} ions possessed a small but nonzero electronic moment, even if this moment did not order magnetically at low temperatures. In this scenario the moment would be too small to lead to observable μ^+ relaxation. The paramagnetic susceptibility of the small-moment state could, however, lead to hyperfine enhancement effects, just as in the case of the nonmagnetic Γ_3 CEF-split ground state. The μSR results could not distinguish between these two possibilities.

The only reasonable mechanism for a small Pr moment is conventional (i.e., spin) Kondo compensation, with a high T_K compared to the temperatures of interest (i.e., $T_K \gg 0.5$ K). An argument similar to that given in Sec. I C for the “traditional” CEF-state hyperfine enhancement leads to similar conclusions, viz., that an enhancement factor $K \approx 10$ requires $T_K \sim 50$ K. We noted above in Sec. III A that a high value of T_K is also necessary for the weak-moment spin-freezing scenario, since incomplete Kondo compensation is the only reasonable way in which the Pr^{3+} ionic moment could be so strongly suppressed. (Our data rule out spin freezing with an ordered moment greater than $3\text{--}4 \times 10^{-3} \mu_B$.)

But the Pr^{3+} $4f$ level lies well below the Fermi energy in all Pr-based metals, a circumstance that drastically reduces the strength of the Kondo coupling and makes such a high T_K extremely unlikely. Furthermore, $T_K \sim 50$ K is of the same order as the energy of the first Pr^{3+} CEF splitting in PrInAg₂ found in neutron-scattering studies.² A Kondo temperature of this magnitude would broaden the CEF levels significantly, contrary to the neutron-scattering results, and also contrary to high-temperature specific-heat data¹ that agree closely with the prediction from the CEF-split level scheme. In addition, as discussed above, the spin entropy is largely removed from Kondo-compensated local moments at temperatures low compared to T_K , and thus the full $R \ln 2$ entropy seen below 1 K (Ref. 1) cannot be accounted for. Thus the high- T_K scenario is not supported by the observed thermal and magnetic properties of PrInAg₂.

D. Effect of muon charge on Pr^{3+} ions

In addition to contributing an electric-field gradient at near-neighbor nuclear sites, the μ^+ charge produces an elec-

tric field that perturbs the CEF splitting of Pr^{3+} near neighbors. The symmetry of these Pr^{3+} sites is lowered and some degeneracies, including that of the Γ_3 ground-state doublet, are lifted. The corresponding modification of the Van Vleck susceptibility has been observed by transverse-field μSR (TF- μSR) in a number of Pr-based intermetallics.^{30,31} The ground-state singlet is, however, still nonmagnetic, and Van Vleck paramagnetism and the corresponding nuclear hyperfine enhancement will remain features of the perturbed system.

If the Pr^{3+} ground state were magnetic (Γ_4, Γ_5), no qualitative effect of the μ^+ charge would be expected except under extreme conditions. If it were argued that in PrInAg₂ the μ^+ electric field splits a magnetic Pr^{3+} ground state so that the perturbed ground state is nonmagnetic, then this perturbation must split the degeneracy by an amount of the order of the unperturbed excitation energy ($\Delta_{\text{CEF}}/k_B \approx 60$ K) to explain the observed temperature dependence of the ZF relaxation (Fig. 4). This would be an improbable coincidence; furthermore, the perturbation would have to be considerably larger than observed previously.^{30–33}

IV. CONCLUSIONS

Two features of the ZF- and LF- μSR results in PrInAg₂ corroborate the conclusion of Yatskar *et al.*¹ that the Kondo behavior of the low-temperature specific heat in this compound originates from an unconventional Kondo effect associated with a nonmagnetic Pr^{3+} Γ_3 CEF ground state. First, the fact that the data show no magnetic anomaly between 100 mK and 10 K rules out both static magnetism and Kondo spin fluctuations associated with a magnetic Pr^{3+} CEF ground state, so that neither of these mechanisms can be responsible for the low-temperature specific-heat anomaly.

Second, the low-temperature μ^+ spin dynamics can be understood in terms of nuclear magnetism only; there is no sign of a Pr^{3+} electronic magnetic moment. Furthermore, quantitative agreement is obtained only if the ^{141}Pr nuclear magnetism is hyperfine enhanced, which can occur only if the Pr^{3+} CEF ground state is nonmagnetic. The experimental value of the low-temperature dipolar coupling between μ^+ and ^{141}Pr nuclei is in good agreement with that calculated assuming hyperfine enhancement of the ^{141}Pr nuclear dipole moment.

In addition, the experimental estimate of the coupling between ^{141}Pr nuclei at low temperatures is about three times larger than the value calculated assuming bare dipolar coupling between ^{141}Pr nuclei. This strongly suggests the existence of an indirect coupling mechanism between ^{141}Pr nuclei that arises from hyperfine enhancement. The required value of the electronic exchange interaction between Pr^{3+} ions ($\mathcal{J}_{\text{el}}/k_B \approx 0.2$ K) is comparable to that in similar Pr-based compounds with nonmagnetic CEF ground states.

All these results depend crucially on hyperfine enhancement, the presence of which is evidence for the absence of a Pr^{3+} ground-state magnetic moment. We also point out that a complete theory of a nonmagnetic Kondo effect in PrInAg₂ may need to take into account a Pr-Pr exchange coupling that is of the order of the Kondo temperature.

ACKNOWLEDGMENTS

We are grateful to W. P. Beyermann and R. Movshovich for discussing their results with us. One of us (D.E.M.) wishes to thank the staff of the MST-10 group, Los Alamos National Laboratory, for their hospitality during his stay at Los Alamos. This work was supported in part by the U.S. National Science Foundation, Grant Nos. DMR-9418991 (Riverside) and DMR-9510454 (Columbia), and in part by

the U.C. Riverside Academic Senate Committee on Research, the Director for Energy Research, Office of Basic Energy Sciences, U.S. Department of Energy (DOE) (Ames), the Japanese agency NEDO (Columbia), and the Netherlands agencies FOM and NWO (Leiden); and was carried out in part under the auspices of the U.S. DOE (Los Alamos). Ames Laboratory is operated for the U.S. DOE by Iowa State University under Contract No. W-7405-Eng-82.

*Present address: Dept. of Physics and Astronomy, McMaster University, Hamilton, Ontario, Canada L8S 4L8.

- ¹A. Yatskar, W. P. Beyermann, R. Movshovich, and P. C. Canfield, *Phys. Rev. Lett.* **77**, 3637 (1996).
- ²R. M. Galera, J. Pierre, E. Sjaud, and A. P. Murani, *J. Chem. Soc. Chem. Commun.* **97**, 151 (1984).
- ³S. A. Al'tshuler, *Zh. Éksp. Teor. Fiz. Pis'ma Red.* **5**, 209 (1967) [*JETP Lett.* **5**, 167 (1967)].
- ⁴M. A. Teplov, in *Crystal Field Effects in Metals and Alloys*, edited by A. Furrer (Plenum Press, New York, 1977), p. 318.
- ⁵D. L. Cox, *Phys. Rev. Lett.* **59**, 1240 (1987).
- ⁶P. D. Sacramento and P. Schlottman, *Phys. Lett. A* **142**, 245 (1989).
- ⁷D. L. Cox and M. Jarrell, *J. Phys.: Condens. Matter* **8**, 9825 (1996).
- ⁸A. Schenck, *Muon Spin Rotation Spectroscopy: Principles and Applications in Solid State Physics* (Hilger, Bristol, 1985).
- ⁹In the following we show that the ¹⁴¹Pr contribution to muon relaxation in PrInAg₂ is, in fact, dynamic, and thus constitutes an exception to this rule.
- ¹⁰R. Kubo and T. Toyabe, in *Magnetic Resonance and Relaxation*, edited by R. Blinc (North-Holland, Amsterdam, 1967), p. 810.
- ¹¹K. Andres and S. Darack, *Physica B & C* **86-88B**, 1071 (1977).
- ¹²K. Andres and E. Bucher, *Phys. Rev. Lett.* **21**, 1221 (1968).
- ¹³K. Andres, *Cryogenics* **18**, 473 (1978).
- ¹⁴B. Bleaney, *Physica (Utrecht)* **69**, 317 (1973).
- ¹⁵R. S. Hayano, Y. J. Uemura, J. Imazato, N. Nishida, T. Yamazaki, and R. Kubo, *Phys. Rev. B* **20**, 850 (1979).
- ¹⁶We make the strong-coupling approximation as a matter of convenience, since it is easier to treat numerically than the Gaussian-Markovian process originally described by Kubo and Toyabe (Ref. 10), and the quantitative differences are small.
- ¹⁷D. R. Noakes, J. H. Brewer, D. R. Harshman, E. J. Ansaldo, and C. Y. Huang, *Phys. Rev. B* **35**, 6597 (1987).
- ¹⁸T. Matsuzaki, K. Nishiyama, K. Nagamine, T. Yamazaki, M. Senba, J. M. Bailey, and J. H. Brewer, *Phys. Lett. A* **123**, 91 (1987).
- ¹⁹M. R. Crook and R. Cywinski, *J. Phys.: Condens. Matter* **9**, 1149 (1997).
- ²⁰Alternative mechanisms for small-moment spin freezing, such as itinerant magnetism involving Pr moments or exchange-induced magnetism, are very unlikely, due to the weak Pr-moment-conduction-electron hybridization in Pr-based intermetallics.
- ²¹A. P. Ramirez, *Annu. Rev. Mater. Sci.* **24**, 453 (1994).
- ²²J. S. Gardner, S. R. Dunsiger, B. D. Baulin, M. J. P. Gingras, J. E. Greedan, R. F. Kiefl, M. D. Lumsden, W. A. MacFarlane, N. P. Raju, J. E. Sonier, I. Swainson, and Z. Tun, *Phys. Rev. Lett.* **82**, 1012 (1999).
- ²³See, for example, A. Abragam, *The Principles of Nuclear Magnetism* (Oxford University Press, Oxford, 1961), Chap. IV.
- ²⁴O. Hartmann, *Phys. Rev. Lett.* **39**, 832 (1977).
- ²⁵M. Camani, F. N. Gygax, W. Rüegg, A. Schenck, and H. Schilling, *Phys. Rev. Lett.* **39**, 836 (1977).
- ²⁶G. M. Luke, J. H. Brewer, S. R. Kreitzman, D. R. Noakes, M. Celio, R. Kadono, and E. J. Ansaldo, *Phys. Rev. B* **43**, 3284 (1991).
- ²⁷R. Movshovich, A. Yatskar, M. F. Hundley, P. C. Canfield, and W. P. Beyermann, *Phys. Rev. B* **59**, R6601 (1999).
- ²⁸S. M. Myers and A. Narath, *Phys. Rev. B* **9**, 227 (1974).
- ²⁹M. Kubota, H. R. Folle, C. Buchal, R. M. Mueller, and F. Pobell, *Phys. Rev. Lett.* **45**, 1812 (1980).
- ³⁰R. Feyerherm, A. Amato, A. Grayevsky, F. N. Gygax, N. Kaplan, and A. Schenck, *J. Alloys Compd.* **231**, 164 (1995).
- ³¹T. Tashma, A. Amato, A. Grayevsky, F. N. Gygax, M. Pinkpank, A. Schenck, and N. Kaplan, *Phys. Rev. B* **56**, 9397 (1997).
- ³²R. Feyerherm, A. Amato, A. Grayevsky, F. N. Gygax, N. Kaplan, and A. Schenck, *Z. Phys. B: Condens. Matter* **99**, 3 (1995).
- ³³A. Grayevsky, I. Felner, T. Tashma, N. Kaplan, F. Gygax, A. Amato, M. Pinkpank, and A. Schenck, *Hyperfine Interact.* **104**, 73 (1997).